Molecular hydrogen upregulates heat shock response and collagen biosynthesis, and downregulates cell cycles - Meta-analyses of gene expression profiles -

Hiroshi Nishiwaki[1], Mikako Ito[1], Shuto Negishi[1], Sayaka Sobue[2] Masatoshi Ichihara[2], Kinji Ohno[1]

[1]Division of Neurogenetics, Center for Neurological Diseases and Cancer, Nagoya University Graduate School of Medicine, 65 Tsurumai, Showa-ku, Nagoya 466-8550, Japan
[2]Department of Biomedical Sciences, College of Life and Health Sciences, Chubu University, 1200 Matsumoto-cho, Kasugai, 487-8501 Japan

Corresponding author:
E-mail: ohnok@med.nagoya-u.ac.jp (KO)

Short Title: Pathways modulated by molecular hydrogen

Abbreviations: HGT, hypergeometric test; ORA, over-representation analysis; GSEA, gene set enrichment analysis; FCS, functional class scoring; SPIA, signaling pathway impact analysis; PRS, pathway regulation score; PTA, pathway topology-based approach; HW, hydrogen water; RMA, robust multi-array average; EB, empirical Bayes; XPN, cross-platform normalization; DWD, distance weighted discrimination; HS_A, HS_r, and HS_B, hypothesis settings (HS), where genes are differentially expressed in all studies, the majority of studies, and one or more studies, respectively; DEGs, differentially expressed genes; FDR, false-discovery rate.

Keywords: molecular hydrogen; meta-analysis, cross-platform analysis; pathway analysis; heat shock protein;

Graphical abstract

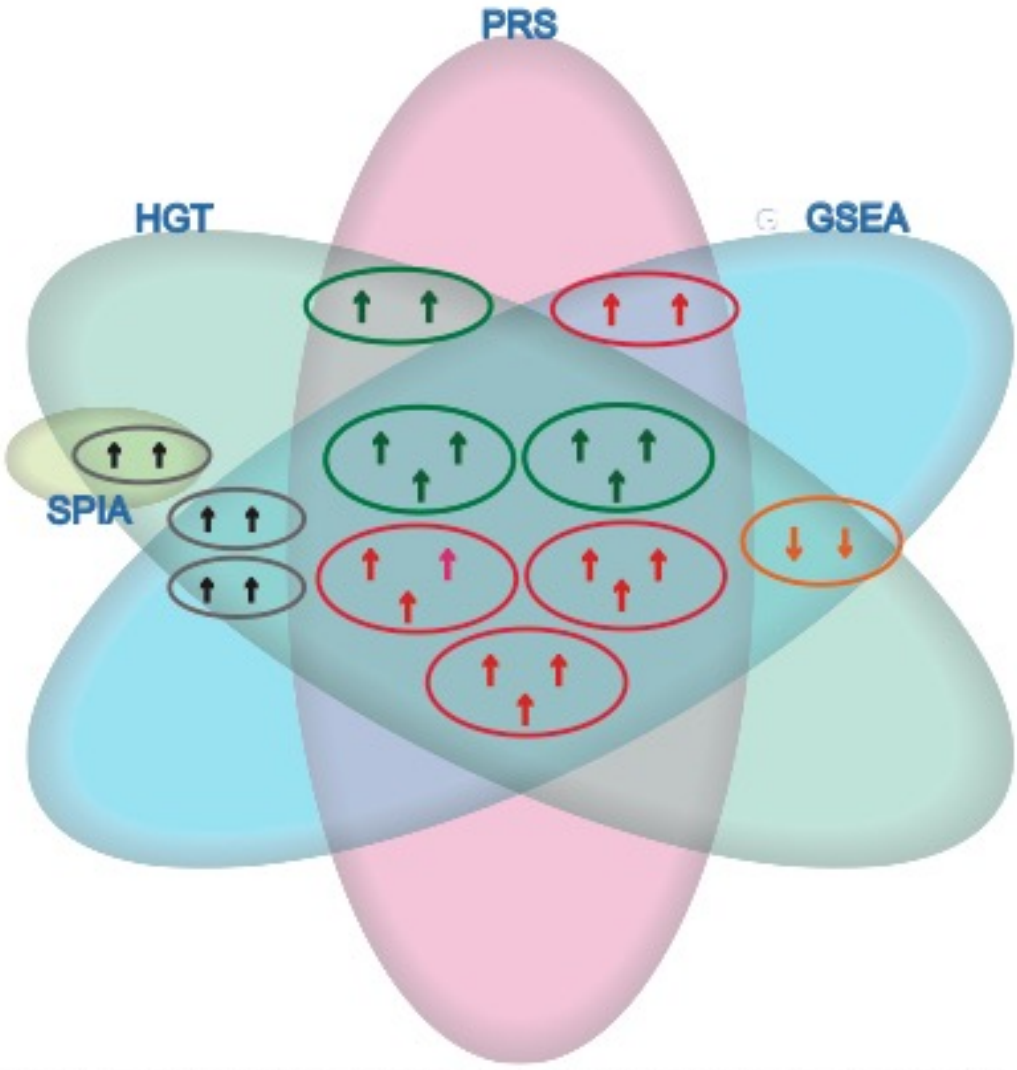

Venn diagram showing pathways detected by different analytical methods. HGT, GSEA, and PRS are different analytical methods. Up- and down-regulated pathways are indicated by upper and lower arrows, respectively. Identical pathways extracted in different analytical methods are indicated by a circle. Green, red, and yellow letter and circles indicate pathways related to "the collagen biosynthesis", "the heat shock response", and "the cell cycles", respectively. Gray circles also indicate pathways, but no features are shared between gray circles.

Abstract

Background: Molecular hydrogen exerts its effect on multiple pathologies, including oxidative stress, inflammation, and apoptosis. However, its molecular mechanisms have not been fully elucidated. In order to explore the effects of molecular hydrogen, we meta-analyzed gene expression profiles modulated by molecular hydrogen.

Methods: We performed microarray analysis of the mouse liver with or without drinking hydrogen water. We also integrated two previously reported microarray datasets of the rat liver into meta-analyses. We used two categories of meta-analysis methods: the cross-platform method and the conventional meta-analysis method (Fisher's method). For each method, hydrogen-modulated pathways were analyzed by (i) the hypergeometric test (HGT) in the class of over-representation analysis (ORA), (ii) the gene set enrichment analysis (GSEA) in the class of functional class scoring (FCS), and (iii) the signaling pathway impact analysis (SPIA), pathway regulation score (PRS), and others in the class of pathway topology-based approach (PTA).

Results: Pathways in the collagen biosynthesis and the heat shock response were upregulated according to (a) ORA with the cross-platform method, (b) GSEA with the cross-platform method, and (c) PRS with the cross-platform method. Pathways in cell cycles were downregulated according to (a) ORA with the cross-platform method, (b) GSEA with the cross-platform method, and (d) GSEA with the conventional meta-analysis method.

Discussion: Because the heat shock response leads to upregulation of collagen biosynthesis and a transient arrest of cell cycles, induction of the heat shock response is likely to be a primary event induced by molecular hydrogen in the liver of wild-type rodents.

Introduction

Since a prominent effect of molecular hydrogen on a rat model of cerebral infarction was reported in 2007[1], more than 300 original articles demonstrated the effects of molecular hydrogen on various pathologies, such as oxidative stress, inflammation, and apoptosis [2,3]. Moreover, clinical benefits of molecular hydrogen in humans have been reported in diabetes mellitus [4], myopathies [5], rheumatoid arthritis [6], hyperlipidemia [7], and Parkinson's disease [8]. Accumulating evidence in rodents and human suggests that molecular hydrogen may ameliorate a diverse array of human diseases.

Hydroxyl radical and peroxynitrite are implicated in the pathology of oxidative stress and inflammation. The effects of molecular hydrogen were initially attributed to the scavenging activities of hydroxyl radical and peroxynitrite [1,9]. However, a short dwell time of exogenously administered hydrogen in our bodies and production of a large amount of hydrogen in our intestine make the radical-scavenging effects of hydrogen unlikely to be the primary mechanism. We have shown that molecular hydrogen inhibits signaling pathways in allergies [10], inflammation [11], and Wnt/β-catenin [12], which require no radical-scavenging effects. Many signaling molecules (for example, Lyn, Ras, JNK, and NF-κB to name a few) are modulated by molecular hydrogen [2,3]. However, the underlying mechanisms of the effects of molecular hydrogen are not fully elucidated.

The effects of molecular hydrogen in disease models have been explored by analyzing gene expression profiles with microarray [13–15]. Gene expression profiles have also been reported in the liver of wild-type rats [15,16]. The rat microarray analysis demonstrates upregulation of genes regulated by histone H3K27 methylation status [15] and of oxidoreduction-related genes [16]. The differences in species, microarray platforms, and the methods of hydrogen administration are likely to account for the difference in the observed results.

Gene expression analysis is largely classified into two types: single-gene analysis and pathway analysis (gene set analysis). Because of multiple comparisons of as many as ~20,000 genes and low detection power due to analysis of single genes, single-gene analysis often fails to detect biological function. In contrast, pathway analysis has fewer numbers of multiple comparisons and higher detection powers compared to single-gene analysis. Because the effects of molecular hydrogen are predicted to be subtle in wild-type rodents, pathway analysis is likely to be suitable for this study.

In order to elucidate the effects of molecular hydrogen on gene expressions, we performed pathway analyses of microarray datasets of the mouse liver with or without drinking hydrogen water. We also integrated two previously reported microarray datasets of the rat liver by us and by others to perform meta-analyses of gene expression profiles modulated by molecular hydrogen. Our meta-analysis pointed to the notion that hydrogen upregulates heat shock response and collagen biosynthesis, and

downregulates cell cycles.

Materials and Methods

Microarray analyses

All animal studies were approved by the Animal Care and Use Committees of Nagoya University and Chubu University. We performed microarray analysis of the wild-type mouse liver treated with molecular hydrogen (dataset #1), and obtained two microarray datasets of the wild-type rat liver, which were previously reported by us (dataset #2) [15] and others (dataset #3) [16] (Supplementary Table 1). As far as we know, no other microarray dataset of the wild-type rodent liver is available for meta-analysis.

In dataset #1, we divided 7-week-old male C57/BL6J mice into two groups: the control group was given dehydrogenized water; and the hydrogen water (HW) group was given hydrogen water that contained 1.4 ppm dissolved hydrogen. Mice had free access to either dehydrogenized or hydrogen water for 4 weeks. After that, mice were sacrificed and RNA was extracted from the whole liver using RNeasy mini kit (Qiagen). Expression profiles were determined by Affymetrix GeneChip Mouse Gene 1.0 ST Array (Santa Clara, CA, USA), which contained 26,166 mouse genes. The experiment was performed exclusively for this communication, and has not been reported before. We posted dataset #1 to the National Center for Biotechnology Information (NCBI) Gene Expression Omnibus (http://www.ncbi.nlm.nih.gov/geo/) with GEO Series ID GSE103941.

In dataset #2, we divided 4-week-old male F344 rats into two groups: the control group was given basal rodent chow and dehydrogenized water, and was housed in room air; and the hydrogen water (HW) group was given basal rodent chow and hydrogen water that contained 1.4 ppm dissolved hydrogen, and was housed in 2% hydrogen gas. Rats had free access to either dehydrogenized or hydrogen water for 3 weeks. After that, rats were sacrificed and RNA was extracted from the whole liver using RNeasy mini kit (Qiagen). Expression profiles were determined by Affymetrix HT RG-230 PM Array, which contained more than 30,000 rat genes. Dataset #2 was used to demonstrate hydrogen-mediated histone modification [15], and was posted to the GEO database with GEO Series ID GSE102868.

Dataset #3 was obtained from the GEO database with GEO Series ID GSE26363 [16]. In dataset #3, 4-week-old male Sprague-Dawley rats were divided into two groups: the control group was given sterilized distilled water and the HW group was given hydrogen water that contained 1.4 ppm dissolved hydrogen. Rats had free access to either sterilized distilled or hydrogen water for 4 weeks. After that, rats were sacrificed and RNA was extracted from the whole liver using RNeasy mini kit (Qiagen). Expression profiles were determined by Affymetrix Rat Genome 230 2.0 Array, which contained more than 30,000 rat genes.

Each raw microarray dataset (CEL files) was normalized with robust multi-array Average (RMA) using the Affymetrix Expression Console Software (Affymetrix).

Preparation of hydrogen water and tissue distribution of molecular hydrogen

In dataset #1, hydrogen water was prepared using Hydrogen Water 7.0 (Ecomo International), which was developed and was kindly provided by MiZ Co. Ltd. The concentration of dissolved hydrogen produced by Hydrogen Water 7.0 was 5–7 ppm. In datasets #2 and #3, hydrogen-rich water (1.4 ppm dissolved hydrogen) was generated from distilled water with 0.44 mM Na_2SO_4 using Aquela Blue, an electrolysis-based device to produce hydrogen-saturated water near neutral pH (MiZ Co. Ltd). In datasets #1 and #2, the dehydrogenized control water was prepared by gently stirring hydrogen-rich water in open air for 24 h.

In dataset #1, the hydrogen concentration decreased from 6-8 ppm to 0.8 ppm in 12 h with a half-life of 1 hour [17]. In datasets #2 and #3, the initial concentration of hydrogen of 1.4 ppm was decreased to 0.6 ppm in 12 h [17]. Rats and mice drink water mostly at night, when the hydrogen concentrations were more than 0.8 ppm (dataset #1) or 0.6 ppm (datasets #2 and #3). As the effects of molecular hydrogen on a rat model of Parkinson's disease were similar among 0.08, 0.5 and 1.5 ppm hydrogen groups [18], we expected that datasets #1, #2, and #3 gave rise to similar gene expression profiles.

Hydrogen water produced by Hydrogen Water 7.0 (dataset #1) and Aquela Blue (datasets #2 and #3) is theoretically free of any contaminants, although the absence of trace contaminants was not scrutinized by us (datasets #1 and #2) or others (dataset #3). In datasets #1 and #2, the control dehydrogenized water was prepared by gently stirring hydrogen-rich water in open air for 24 h. Therefore, the effects of byproducts of molecular hydrogen, if any, are unlikely to affect gene expression profiles. In addition, Molecular hydrogen is a stable gas that can react only with oxide radical ion ($\bullet O^-$) and hydroxyl radical ($\bullet OH$) in water with low reaction rate constants of $\sim 10^7\ M^{-1} \cdot s^{-1}$ [2]. Thus, molecular hydrogen is unlikely to produce byproducts in our body.

We previously reported temporal profiles of concentrations of molecular hydrogen in rat tissues after intragastric administration of 4-ml hydrogen-rich water (1.2-1.6 ppm) [19]. The concentrations of molecular hydrogen in atrial blood increased to its peak of 4 μM in 5 min and returned to the basal level in 30 min. Similarly, the concentrations of molecular hydrogen in the liver increased to its peak of ~10 μM in 5 min and returned to the basal level in 30 min. Higher concentration of molecular hydrogen in the liver was likely to be accounted for by binding of molecular hydrogen to glycogen in the liver [20].

Pathway Database

Pathway datasets were downloaded from the Reactome pathway database (http://www.reactome.org/download/current/ReactomePathways.gmt.zip) [21].

Cross-platform analysis and conventional meta-analysis methods

Although the cross-platform analysis method usually has better performance than the conventional meta-analysis method for the identification of biological functions [22], the efficiencies are different from datasets to datasets. We thus collated the three pairs of datasets using both methods: the cross-platform analysis method and the conventional meta-analysis method (Fig. 1).

The cross-platform method merges all datasets across different microarray platforms into a single dataset. After being merged, a single dataset is subject to pathway analyses. There are three cross-platform methods: the ComBat method employing the empirical Bayes (EB) estimation [23]; the cross-platform normalization (XPN) method [24]; and the distance weighted discrimination (DWD) method [25]. Among them, we adopted the ComBat method [23], encoded in inSilicoMerging, an R/Bioconductor package [26] for the ease of convergence. The integrated dataset was then subject to pathway analyses.

In contrast to the cross-platform method, the conventional meta-analysis method does not merge the datasets in advance. With the conventional meta-analysis method, each microarray dataset is analyzed individually, and *p*-values of the extracted pathways are merged afterwards. The conventional meta-analysis methods used for microarray datasets include six methods that combine *p*-values (Fisher, Stouffer, adaptively weighted Fisher, minP, maxP, and rOP); two methods that combine the effect sizes (FEM and REM), and four methods that combine the ranks (RankProd, RankSum, product of ranks, and sum of ranks) [22,27]. These twelve conventional meta-analysis methods can be classified into three categories on the basis of the hypothesis settings (HS). The three categories are based on whether genes are differentially expressed in all studies (HS_A), the majority of studies (HS_r), or one or more studies (HS_B). HS_A includes product of ranks, sum of ranks, and maxP. HS_r includes rOP and REM. HS_B includes Fisher, adaptively weighted Fisher, Stouffer, minP, RankProd, RankSum, and FEM. To analyze microarray datasets with different platforms obtained from mice and rats treated with different hydrogen administration protocols, we adopted the commonly used Fisher's method in the category of HS_B, which dominates in simplicity, detection power, and biological association [27]. In the Fisher's method, one-tailed *p*-values of pathways or genes in the direction of up-regulation are calculated for each microarray dataset. An integrated *p*-value in the direction of up-regulation is calculated by $-2\sum_{i=1}^{n}\ln p_i$ (p_i is one-tailed *p*-value for the i^{th} hypothesis test). Similarly, an integrated *p*-value in the direction of down-regulation is calculated. The integrated *p*-value follows the chi-square distribution of *2n* degrees of freedom.

Pathway analyses

Pathway analyses can be classified into three classes: over-representation analysis (ORA), functional class scoring (FCS), and pathway topology-based approach (PTA). ORA, FCS, and PTA are historically and functionally the first, second, and third generations of pathway analyses, respectively. The first generation ORA determines differentially expressed genes (DEGs) individually, and only gene names of DEGs are taken into account. In contrast, the second generation FCS does not determine DEGs, but takes into account the fold-changes of individual genes. The third generation PTA considers pathway structures in addition to the features used in FCS [28,29].

A total of nine pathway analyses have been reported in these three classes: (i) the hypergeometric test (HGT) in the class of ORA [30–33], (ii) the gene set enrichment analysis (GSEA) [34] in the class of FCS, and (iii) the signaling pathway impact analysis (SPIA) [35], the pathway regulation score (PRS) [36], Clipper [37], DEGraph [38], TopologyGSA [39], TAPPA [40], and PWEA [41] in the class of PTA (Fig. 1). These nine pathway analyses were variably applied to the cross-plat form analysis method and to the conventional meta-analysis method (Fig. 1).

Analytical methods in the class of PTA, except for PRS (PTA), consider pathway structure and allow up- and down-regulation of gene expressions in a single pathway, which is an advantage of PTA compared to the first generation ORA and the second generation FCS. In the conventional meta-analysis (Fisher's method), integrated *p*-values need to be calculated in each direction of up- and down-regulation separately. Thus, the Fisher's method could not be applied to PTA. Among analytic methods in PTA, however, PRS (PTA) only takes into account up-regulated genes. We thus conducted the conventional meta-analysis with the Fisher's method for HGT (ORA), GSEA (FCS), and PRS (PTA) (Fig. 1).

In the class of the first generation ORA, HGT was conducted using ConsensusPathDB [42]. With the cross-platform method, we performed *t*-tests for expression levels of each gene for the integrated dataset, and extracted up- and down-regulated genes with p-values < 0.05, respectively. The genes up- and down-regulated by molecular hydrogen were tested, respectively, using ConsensusPathDB. With the conventional meta-analysis method (Fisher's method), we performed *t*-tests for expression levels of each gene for individual datasets, and extracted up- and down-regulated genes with p-values < 0.05 or < 0.10. The up- and down-regulated genes were similarly tested for each microarray dataset using ConsensusPathDB. The integrated *p*-value was calculated afterwards.

In the class of the second generation FCS, GSEA was conducted using javaGSEA desktop application (http://software.broadinstitute.org/gsea/downloads.jsp). With the cross-platform method, we conducted GSEA using the integrated dataset. With the conventional meta-analysis method (Fisher's method), we conducted GSEA using each microarray dataset. *P*-value of 0 generated by GSEA was set to 0.001, because

p-value of 0 stands for no occurrence in 1000 permutations. With GSEA, one-tailed *p*-value (*p*) was calculated for each gene set. When the enrichment score in the direction of upregulation is more than that in the direction of downregulation in a specific gene set, the *p*-value in the up-direction was set to *p*, and the *p*-value in the down-direction was expediently set to 1. Two integrated *p*-values were calculated for each gene set in the directions of up- and down-regulations. Statistical significance was estimated after Bonferroni correction.

In the class of the third generation PTA, Clipper was conducted using graphite, an R/Bioconductor package [43]. SPIA, DEGraph, TopologyGSA, TAPPA, PRS, and PWEA were conducted using ToPASeq, an R/Bioconductor package [44].

Statistical thresholds

In the cross-platform method, the false-discovery rate (FDR, *q*-value) was calculated using the Benjamini and Hochberg method except GSEA. In GSEA, the false-discovery rate (FDR, *q*-value) was calculated by GSEA, which took into account the number of genes in each geneset. We arbitrarily set the threshold of *q*-value to < 1/8 to obtain decent numbers of pathways. In Clipper, pathways with both $\alpha_{mean} < 0.05$ (*p*-value for the mean which is calculated on the basis of graphical Gaussian model) and $\alpha_{var} < 0.05$ (*p*-value for the inverse covariance matrix which is calculated on the basis of graphical Gaussian model) were considered. In the conventional meta-analysis method (Fisher's method), we applied Bonferroni correction to the integrated *p*-values.

Results

Single-gene analysis

We first looked into single genes that were changed by molecular hydrogen in each dataset, and converged *p*-values by the Fisher's method for conventional meta-analysis. None of the converged *p*-values was less than 0.05 after Bonferroni correction. Similarly, the cross-platform analysis method detected no genes with *p*-values less than 0.05 after Bonferroni correction.

Pathway analyses

As single-gene analysis detected no genes that were changed by molecular hydrogen, we next employed nine different analytical methods of pathway analysis (Fig. 1). The numbers of detected pathways are summarized in Table 1, and the results are graphically shown in Fig. 2.

Pathway analysis 1: HGT in the class of the first generation ORA

Cross-platform analysis of upregulated genes with HGT (ORA) revealed that 14 Reactome pathways were enriched in the direction of upregulation (Table 2). The top

two pathways were “collagen biosynthesis and modifying enzymes” and “collagen formation”. The 6th pathway was also related to collagen biosynthesis. The 7th, 10th, and 12th pathways were related to the heat shock response. On the other hand, the cross-platform analysis of downregulated genes with HGT (ORA) revealed that three Reactome pathways were enriched in the direction of downregulation (Table 2). The three pathways were all related to the cell cycles.

Meta-analysis with HGT (ORA) revealed that all integrated *p*-values of Reactome pathways were higher than 0.05 after Bonferroni corrections in the directions of both up- and down-regulation.

Pathway analysis 2: GSEA in the class of the second generation FCS

Cross-platform analysis detected nine upregulated Reactome pathways (Table 3). The 1st, 2nd, 3rd, and 8th pathways were related to the heat shock response. Among these, the 2nd, 3rd, and 8th pathways were also detected with HGT (ORA) stated above. The 5th and 9th pathways were related to the collagen biosynthesis, and were also detected with HGT (ORA). Similarly, nine Reactome pathways were downregulated (Table 3). Out of the nine pathways, seven pathways were related to the cell cycles.

Meta-analysis detected eight downregulated Reactome pathways, which were related to the cell cycles (Table 4).

Pathway analysis 3: The class of the third generation PTA

PTA takes into account the pathway structures [28,29]. In contrast to ORA and FCS, PTA is designed to detect a pathway, in which activation of an upstream gene causes both upregulation of a subset of downstream genes and downregulation of another subset of downstream genes. Two datasets may exhibit opposite effects on an identical pathway. With ORA and FCS, we can integrate such *p*-values, because up- and down-regulations of a pathway are taken into account individually. In contrast, with PTA, we cannot integrate such *p*-values, because up- and down-regulations cannot be discriminated. The analytical method, PRS in the class of PTA, however, is exceptional, because PRS analyzes only upregulated genes. We therefore used cross-platform analysis for all analytical methods (SPIA, Clipper, PRS, DEGraph, TopologyGSA, TAPPA, and PWEA) in PTA, and conventional meta-analysis only for PRS in PTA.

Pathway analysis 3a: SPIA in the class of the third generation PTA

SPIA analysis detected one Reactome pathway, “Extracellular matrix organization”, which is a superset of “collagen biosynthesis and modifying enzymes” and “collagen formation”.

Pathway analysis 3b: Clipper in the class of the third generation PTA

Clipper analysis detected six Reactome pathways (Table 5). These pathways

were unique to Clipper, and were not detected in other analyses.

Pathway analysis 3c: PRS in the class of the third generation PTA

PRS disclosed nine Reactome pathways (Table 6). The 1st and 2nd, 9th pathways were relevant to the collagen biosynthesis. The 1st and 2nd pathways were also observed in HGT (ORA) and GSEA (FCS). The 3rd and 4th, 7th, 8th pathways were related to the heat shock response. Three out of the four pathways were also extracted in HGT (ORA) and GSEA (FCS).

Pathway analyses 3d, 3e, 3f, and 3g: DEGraph, TopologyGSA, TAPPA, and PWEA in the class of the third generation PTA

No pathways were significantly changed.

Discussion

We performed nine analytical methods with cross-platform analysis and three analytical methods with conventional meta-analysis (Fig. 1). We obtained hydrogen-modulated pathways in five methods with cross-platform analysis and one method with conventional meta-analysis (Table 1). Pathways in (i) the heat shock response, (ii) the collagen biosynthesis, and (iii) the cell cycles were shared among different analytical methods.

When analytical methods with the cross-platform analysis were compared, HGT (ORA), GSEA (FCS), and PRS (PTA) detected almost identical pathways in the collagen biosynthesis and the heats hock response in the direction of upregulation. In addition, HGT (ORA) and GSEA (FCS), but not PRS (PTA), detected similar pathways in the cell cycles in the direction of downregulation. PRS (PTA) failed to detect pathways in the cell cycles, which was likely because PRS was designed to detect upregulated pathways [36]. In contrast to PRS (PTA), the other six analytical methods (SPIA, Clipper, DEGraph, TopologyGSA, TAPPA, and PWEA) in the class of PTA take into account both up- and down-regulated genes. However, SPIA (PTA) and Clipper (PTA) detected one and six pathways, respectively; and DEGraph (PTA), TopologyGSA (PTA), TAPPA (PTA), and PWEA (PTA) detected none. There are three possible reasons for less productive results with the PTA methods except Clipper. One possibility is that the modulation of gene expression levels induced by molecular hydrogen was too subtle to be detected by the six PTA methods. Another possibility is that these PTA methods are designed to analyze single platform data and variabilities in our three platforms spoiled the advantages of the six PTA methods. The third possibility is that integration of both up- and down-regulated genes in a single analysis has somehow abolished the advantage of incorporation of the pathway structures in the six PTA methods. Although GSEA also uses both up- and down-regulated genes in a single analysis, the up- and down-regulated genes are not integrated together as in the six PTA

methods. Instead, ranks of either up- or down-regulated genes, but not both, determine the statistical significance in GSEA (FCS). Among the six PTA methods, only Clipper (PTA) detected as many as six pathways, which, however, were different from pathways detected by HGT (ORA), GSEA (FCS), and PRS (PTA). In contrast to shared features in pathways detected by HGT (ORA), GSEA (FCS), and PRS (PTA), the six pathways detected by Clipper (PTA) were dissimilar to those detected by the three methods. Clipper (PTA) integrates both up- and down-regulated genes, which made pathways extracted by Clipper (PTA) different from those extracted by HGT (ORA), GSEA (FCS), and PRS (PTA).

Upregulation of genes in the heat shock response was detected in HGT (ORA), GSEA (FCS), and PRS (PTA). Indeed, expressions of most genes in the "attenuation phase", which is one of pathways in the heat shock response, were upregulated (Fig. 3), although none of these genes were detected by single-gene analysis. As the activated heat shock response provokes a transient arrest of cell cycles [45] and facilitates collagen biosynthesis [46], upregulation of the heat shock response is likely to be a primary event among the three extracted pathways. HSP47 (*SERPINH1*) is a collagen-binding glycoprotein in the endoplasmic reticulum expressed only in collagen-producing cells, and serves as a molecular chaperone essential for formation of collagens I-V [46]. Expression of HSP47 is tightly correlated with the collagen expression [46]. Indeed, we observed in our datasets that *SERPINH1* (HSP47) and genes for collagen type I-V were upregulated (Supplementary Table 2, 3). Overexpression of HSP70 is effective for myocardial ischemia and brain ischemia [47,48]. In our datasets, genes for HSP70 were upregulated (Supplementary Table 4). Therefore, the effects of molecular hydrogen on rat models of myocardial infarction [49,50] and cerebral infarction [1] were likely to be partly accounted for by upregulation of HSP70. The balance between HSP90 and HSP70 is associated with adult onset neurodegenerative diseases [51,52]. HSP90 stabilizes the client proteins and inhibits their ubiquitination, while HSP70 promotes ubiquitination and proteasomal degradation. In our datasets, genes encoding HSP70s were upregulated by hydrogen (Supplementary Table 4), whereas genes for HSP90s were either up- or down-regulated (Supplementary Table 5). The effects of molecular hydrogen on Parkinson's disease [8,53] and Alzheimer's disease [54,55] may be partly attributed to the relative upregulation of HSP70.

In this study, gene expression profiles were determined in the whole liver in all the datasets. Thus, contributions of parenchymal and non-parenchymal cells of the liver to gene expression profiles could not be dissected in any datasets. Kupffer cells are activated by hepatic ischemia-reperfusion in rats [56] and by LPS in cultured cells [57,58]. Under the hypothermic condition, carbon monoxide gas upregulates HSP70 and inhibits the production of ROS in Kupffer cells [59]. Similarly, we previously reported that hydrogen upregulates HSP70 in the mouse liver [15]. Considering that molecular hydrogen is a mitohormetic effector [60], it is likely that molecular hydrogen induced

the heat shock response in Kupffer cells as observed in carbon monoxide. In general, Kupffer cells release cytokines such as IL-6 and TNF-α, and transduce signals to the hepatocytes and the hepatic stellate cells [58]. Kupffer cells stimulated by LPS promote collagen accumulation in the hepatic stellate cells [57]. Similar mechanisms are likely to be functional in the liver treated with molecular hydrogen. As the heat shock response leads to transient arrest of cell cycles in mammalian cells [45], the heat shock response induced by molecular hydrogen is likely to lead to cell cycle arrest in Kupffer cells.

Author contributions

HN and KO conceived the study; HN performed *in silico* studies; MiI, SS, and MaI performed microarray analyses; HN, MiI, SN, and KO discussed biological significance of observations and wrote the manuscript. All authors read and approved the final version of the manuscript.

Conflicts of interest

The authors declare no conflicts of interest.

Acknowledgements

This study was supported by Grants-in-Aids from the Ministry of Education, Culture, Sports, Science, and Technology of Japan (15H04840, 15K06812, and 26870682); the Ministry of Health, Labour, and Welfare of Japan (H29-Nanchi-Ippan-030); the Japan Agency for Medical Research and Development (17ek0109230h0001 and 17gm1010002h0002); the Intramural Research Grant from NCNP (29-4), and the Chubu University Grant (29IM17A, 29IM37A, and 29IM08B).

References

[1] Ohsawa I, Ishikawa M, Takahashi K, et al. Hydrogen acts as a therapeutic antioxidant by selectively reducing cytotoxic oxygen radicals. Nat Med 2007;13:688–94.

[2] Ohno K, Ito M, Ichihara M, et al. Molecular hydrogen as an emerging therapeutic medical gas for neurodegenerative and other diseases. Oxid Med Cell Longev 2012;

[3] Ichihara M, Sobue S, Ito M, et al. Beneficial biological effects and the underlying mechanisms of molecular hydrogen - comprehensive review of 321 original articles. Med Gas Res 2015;5:12.

[4] Kajiyama S, Hasegawa G, Asano M, et al. Supplementation of hydrogen-rich water improves lipid and glucose metabolism in patients with type 2 diabetes or impaired glucose tolerance. Nutr Res 2008;28:137–143.

[5] Ito M, Ibi T, Sahashi K, et al. Open-label trial and randomized, double-blind, placebo-controlled, crossover trial of hydrogen-enriched water for mitochondrial and inflammatory myopathies. Med Gas Res 2011;1:24.

[6] Ishibashi T, Sato B, Rikitake M, et al. Consumption of water containing a high concentration of molecular hydrogen reduces oxidative stress and disease activity in patients with rheumatoid arthritis: an open-label pilot study. Med Gas Res 2012;2:27.

[7] Song G, Lin Q, Zhao H, et al. Hydrogen activates atp-binding cassette transporter a1-dependent efflux ex vivo and improves high-density lipoprotein function in patients with hypercholesterolemia: A double-blinded, randomized, and placebo-controlled trial. J Clin Endocrinol Metab 2015;100:2724–2733.

[8] Yoritaka A, Takanashi M, Hirayama M, et al. Pilot study of H_2 therapy in Parkinson's disease: a randomized double-blind placebo-controlled trial. Mov Disord 2013;28:836–9.

[9] Ohta S. Molecular hydrogen is a novel antioxidant to efficiently reduce oxidative stress with potential for the improvement of mitochondrial diseases. Biochim Biophys Acta - Gen Subj 2012;1820:586–594.

[10] Itoh T, Fujita Y, Ito M, et al. Molecular hydrogen suppresses FcepsilonRI-mediated signal transduction and prevents degranulation of mast cells. Biochem Biophys Res Commun 2009;389:651–6.

[11] Itoh T, Hamada N, Terazawa R, et al. Molecular hydrogen inhibits lipopolysaccharide/interferon gamma-induced nitric oxide production through modulation of signal transduction in macrophages. Biochem Biophys Res Commun 2011;411:143–149.

[12] Lin Y, Ohkawara B, Ito M, et al. Molecular hydrogen suppresses activated Wnt/β-catenin signaling. Sci Rep 2016;6:31986.

[13] Iuchi K, Imoto A, Kamimura N, et al. Molecular hydrogen regulates gene expression by modifying the free radical chain reaction-dependent generation of

oxidized phospholipid mediators. Sci Rep 2016;6:18971.

[14] Kamimura N, Ichimiya H, Iuchi K, et al. Molecular hydrogen stimulates the gene expression of transcriptional coactivator PGC-1α to enhance fatty acid metabolism. Npj Aging Mech Dis 2016;2:16008.

[15] Sobue S, Inoue C, Hori F, et al. Biochemical and Biophysical Research Communications Molecular hydrogen modulates gene expression via histone modi fi cation and induces the mitochondrial unfolded protein response. Biochem Biophys Res Commun 2017;1–7.

[16] Nakai Y, Sato B, Ushiama S, et al. Hepatic oxidoreduction-related genes are upregulated by administration of hydrogen-saturated drinking water. Biosci Biotechnol Biochem 2011;75:774–776.

[17] Hasegawa S, Ito M, Fukami M, et al. Molecular hydrogen alleviates motor deficits and muscle degeneration in mdx mice. Redox Rep 2017;22:26–34.

[18] Fujita K, Seike T, Yutsudo N, et al. Hydrogen in drinking water reduces dopaminergic neuronal loss in the 1-methyl-4-phenyl-1,2,3,6-tetrahydropyridine mouse model of Parkinson's disease. PLoS One 2009;4:.

[19] Sobue S, Yamai K, Ito M, et al. Simultaneous oral and inhalational intake of molecular hydrogen additively suppresses signaling pathways in rodents. Mol Cell Biochem 2015;403:231–241.

[20] Kamimura N, Nishimaki K, Ohsawa I, et al. Molecular hydrogen improves obesity and diabetes by inducing hepatic FGF21 and stimulating energy metabolism in db/db mice. Obesity 2011;19:1396–1403.

[21] Fabregat A, Sidiropoulos K, Garapati P, et al. The reactome pathway knowledgebase. Nucleic Acids Res 2016;44:D481–D487.

[22] Walsh C, Hu P, Batt J, et al. Microarray Meta-Analysis and Cross-Platform Normalization: Integrative Genomics for Robust Biomarker Discovery. Microarrays 2015;4:389–406.

[23] Johnson WE, Li C, Rabinovic A. Adjusting batch effects in microarray expression data using empirical Bayes methods. Biostatistics 2007;8:118–27.

[24] Shabalin AA, Tjelmeland H, Fan C, et al. Merging two gene-expression studies via cross-platform normalization. Bioinformatics 2008;24:1154–1160.

[25] Benito M, Parker J, Du Q, et al. Adjustment of systematic microarray data biases. Bioinformatics 2004;20:105–114.

[26] Taminau J, Meganck S, Lazar C, et al. Unlocking the potential of publicly available microarray data using inSilicoDb and inSilicoMerging R/Bioconductor packages. BMC Bioinformatics 2012;13:335.

[27] Chang L-C, Lin H-M, Sibille E, et al. Meta-analysis methods for combining multiple expression profiles: comparisons, statistical characterization and an application guideline. BMC Bioinformatics 2013;14:368.

[28] Khatri P, Sirota M, Butte AJ. Ten years of pathway analysis: Current approaches and outstanding challenges. PLoS Comput Biol 2012;8:.

[29] Jin L, Zuo X-Y, Su W-Y, et al. Pathway-based analysis tools for complex diseases: a review. Genomics Proteomics Bioinformatics 2014;12:210–20.

[30] Khatri P, Draghici S, Ostermeier GC, et al. Profiling gene expression using onto-express. Genomics 2002;79:266–70.

[31] Drăghici S, Khatri P, Martins RP, et al. Global functional profiling of gene expression. Genomics 2003;81:98–104.

[32] Berriz GF, King OD, Bryant B, et al. Characterizing gene sets with FuncAssociate. Bioinformatics 2003;19:2502–2504.

[33] Beißbarth T, Speed TP. GOstat: Find statistically overrepresented Gene Ontologies with a group of genes. Bioinformatics 2004;20:1464–1465.

[34] Subramanian A, Tamayo P, Mootha VK, et al. Gene set enrichment analysis: a knowledge-based approach for interpreting genome-wide expression profiles. Proc Natl Acad Sci U S A 2005;102:15545–50.

[35] Tarca AL, Draghici S, Khatri P, et al. A novel signaling pathway impact analysis. Bioinformatics 2009;25:75–82.

[36] Ibrahim MA-H, Jassim S, Cawthorne MA, et al. A Topology-Based Score for Pathway Enrichment. J Comput Biol 2012;19:563–573.

[37] Martini P, Sales G, Massa MS, et al. Along signal paths: An empirical gene set approach exploiting pathway topology. Nucleic Acids Res 2013;41:.

[38] Jacob L, Neuvial P, Dudoit S. More power via graph-structured tests for differential expression of gene networks. Ann Appl Stat 2012;6:561–600.

[39] Massa MS, Chiogna M, Romualdi C. Gene set analysis exploiting the topology of a pathway. BMC Syst Biol 2010;4:121.

[40] Gao S, Wang X. TAPPA: Topological analysis of pathway phenotype association. Bioinformatics 2007;23:3100–3102.

[41] Hung J-H, Whitfield TW, Yang T-H, et al. Identification of functional modules that correlate with phenotypic difference: the influence of network topology. Genome Biol 2010;11:R23.

[42] Kamburov A, Stelzl U, Lehrach H, et al. The ConsensusPathDB interaction database: 2013 Update. Nucleic Acids Res 2013;41:.

[43] Sales G, Calura E, Cavalieri D, et al. graphite - a Bioconductor package to convert pathway topology to gene network. BMC Bioinformatics 2012;13:20.

[44] Ihnatova I, Budinska E. ToPASeq: an R package for topology-based pathway analysis of microarray and RNA-Seq data. BMC Bioinformatics 2015;16:350.

[45] Kühl NM, Rensing L. Heat shock effects on cell cycle progression. Cell Mol Life Sci 2000;57:450–463.

[46] Ishida Y, Nagata K. Hsp47 as a collagen-specific molecular chaperone. Methods Enzymol 2011;499:167–182.

[47] Marber MS, Mestril R, Chi SH, et al. Overexpression of the rat inducible 70-kD heat stress protein in a transgenic mouse increases the resistance of the heart to ischemic injury. J Clin Invest 1995;95:1446–1456.

[48] Dubey A, Prajapati KS, Swamy M, et al. Heat shock proteins: A therapeutic target worth to consider. Vet World 2015;8:46–51.

[49] Hayashida K, Sano M, Ohsawa I, et al. Inhalation of hydrogen gas reduces infarct size in the rat model of myocardial ischemia-reperfusion injury. Biochem Biophys Res Commun 2008;373:30–35.

[50] Zhang G, Gao S, Li X, et al. Pharmacological postconditioning with lactic acid and hydrogen rich saline alleviates myocardial reperfusion injury in rats. Sci Rep 2015;5:9858.

[51] Pratt WB, Gestwicki JE, Osawa Y, et al. Targeting Hsp90/Hsp70-based protein quality control for treatment of adult onset neurodegenerative diseases. Annu Rev Pharmacol Toxicol 2015;55:353–71.

[52] Peng HM, Morishima Y, Pratt WB, et al. Modulation of heme/substrate binding cleft of neuronal nitric-oxide synthase (nNOS) regulates binding of Hsp90 and Hsp70 proteins and nNOS ubiquitination. J Biol Chem 2012;287:1556–1565.

[53] Fu Y, Ito M, Fujita Y, et al. Molecular hydrogen is protective against 6-hydroxydopamine-induced nigrostriatal degeneration in a rat model of Parkinson's disease. Neurosci Lett 2009;453:81–85.

[54] Li J, Wang C, Zhang JH, et al. Hydrogen-rich saline improves memory function in a rat model of amyloid-beta-induced Alzheimer's disease by reduction of oxidative stress. Brain Res 2010;1328:152–161.

[55] Wang C, Li J, Liu Q, et al. Hydrogen-rich saline reduces oxidative stress and inflammation by inhibit of JNK and NF-kappaB activation in a rat model of amyloid-beta-induced Alzheimer's disease. Neurosci Lett 2011;491:127–132.

[56] Kobayashi T, Hirano K, Yamamoto T, et al. The protective role of Kupffer cells in the ischemia-reperfused rat liver. Arch Histol Cytol 2002;65:251–261.

[57] Zhang X, Yu WP, Gao L, et al. Effects of lipopolysaccharides stimulated Kupffer cells on activation of rat hepatic stellate cells. World J Gastroenterol 2004;10:610–613.

[58] Dixon LJ, Barnes M, Tang H, et al. Kupffer cells in the liver. Compr Physiol 2013;3:785–797.

[59] Lee LY, Kaizu T, Toyokawa H, et al. Carbon monoxide induces hypothermia tolerance in Kupffer cells and attenuates liver ischemia/reperfusion injury in rats. Liver Transplant 2011;17:1457–1466.

[60] Murakami Y, Ito M, Ohsawa I. Molecular hydrogen protects against neuroblastoma cell death through the process of mitohormesis. 2017;1–14.

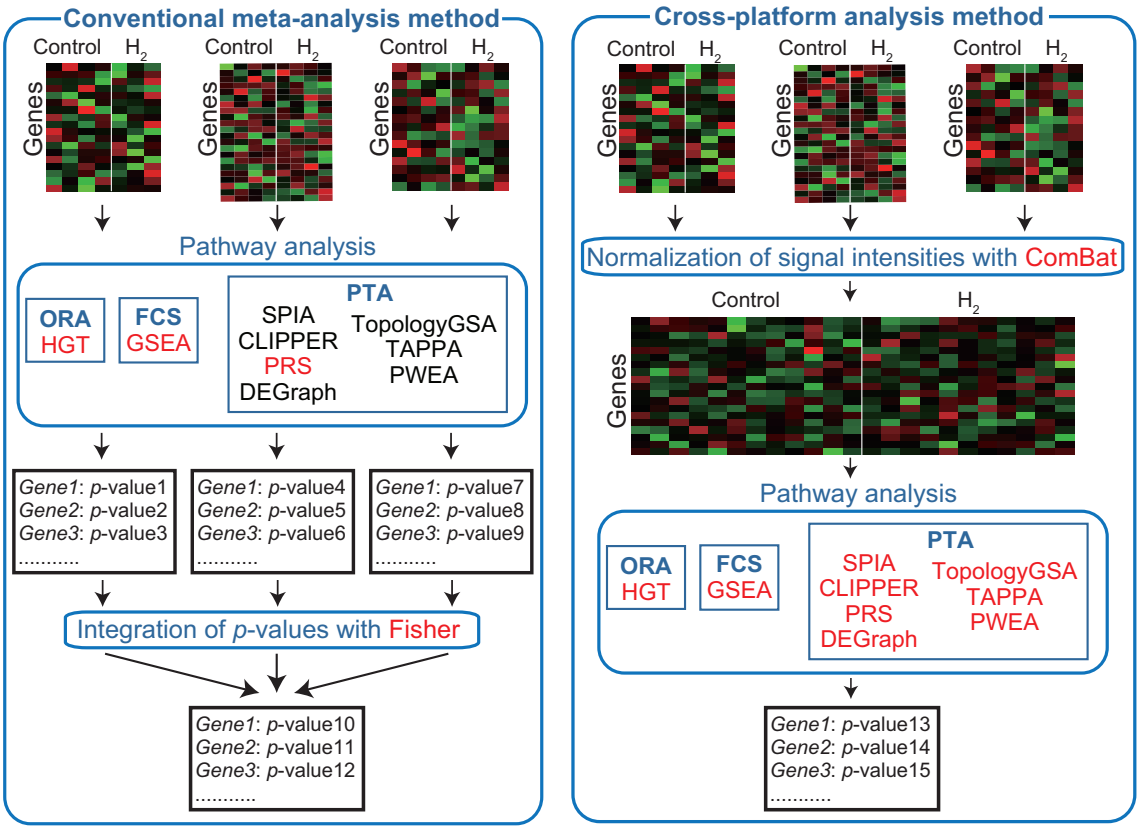

Figure. 1. Schematic of analytical procedures. In conventional meta-analysis, *p*-values were calculated for each dataset using three analytical methods indicated in red. *P*-values of three datasets for each pathway were integrated by the Fisher's method. In cross-platform analysis, signal intensities of three datasets were normalized by ComBat. The normalized signal intensities across three datasets were subject to nine analytical methods indicated in red.

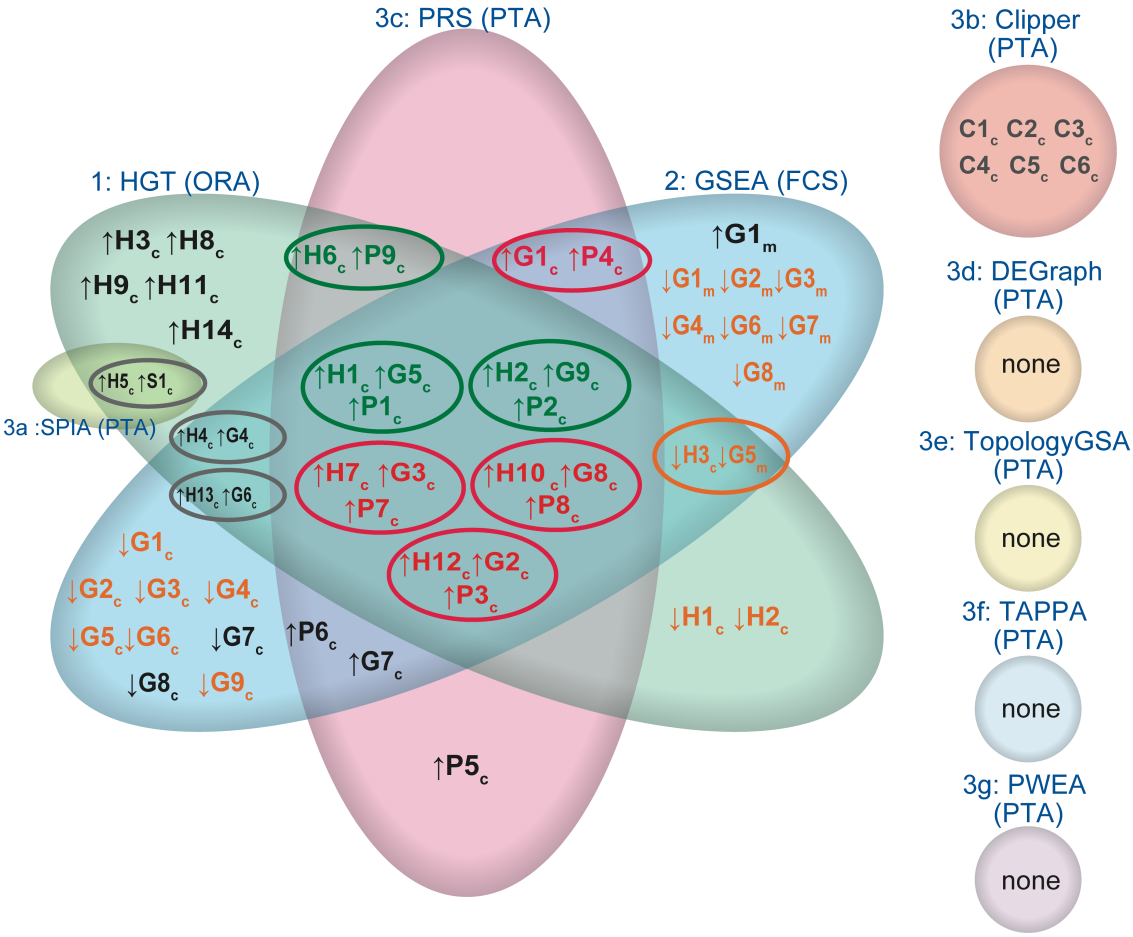

Figure. 2. Venn diagram showing pathways detected by different analytical methods shown in Tables 2 to 6. Up- and down-regulated pathways are indicated by upper and lower arrows, respectively. Clipper integrates up- and down-regulated genes in a single analysis, and arrows are not indicated for Clipper. The name of pathway is indicated by [HGSCP][1-14][$_{cm}$]: H, G, S, C, and P indicate HGT (ORA) (Table 2), GSEA (FCS) (Table 3), SPIA (PTA) (Table 4), Clipper (PTA) (Table 5), and PRS (PTA) (Table 6), respectively; 1-12 indicate the rank in each method; and subscripted "c" and "m" indicate cross-platform analysis and conventional meta-analysis, respectively. Identical pathways extracted in different analytical methods are gathered in a circle. Green, red, and yellow letters and circles indicate pathways related to "the collagen biosynthesis", "the heat shock response", and "the cell cycles", respectively. Gray circles also indicate identical pathways, but have no shared features with other circled pathways.

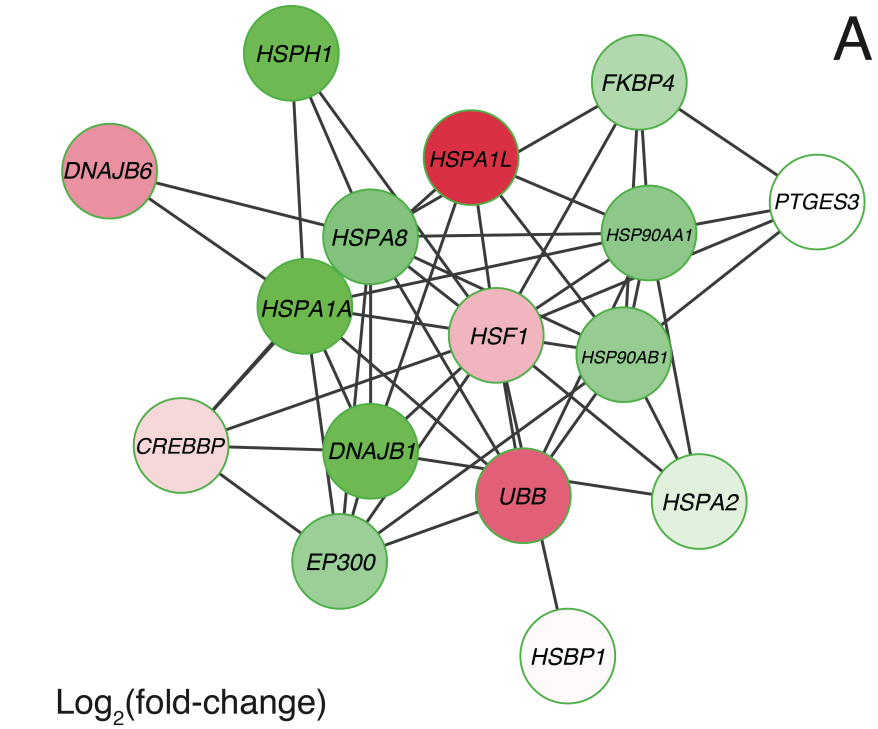
A
HSPH1
FKBP4
DNAJB6
HSPA1L
PTGES3
HSPA8
HSP90AA1
HSPA1A
HSF1
HSP90AB1
CREBBP
DNAJB1
UBB
HSPA2
EP300
HSBP1
Log2(fold-change)
-0.06
0.28

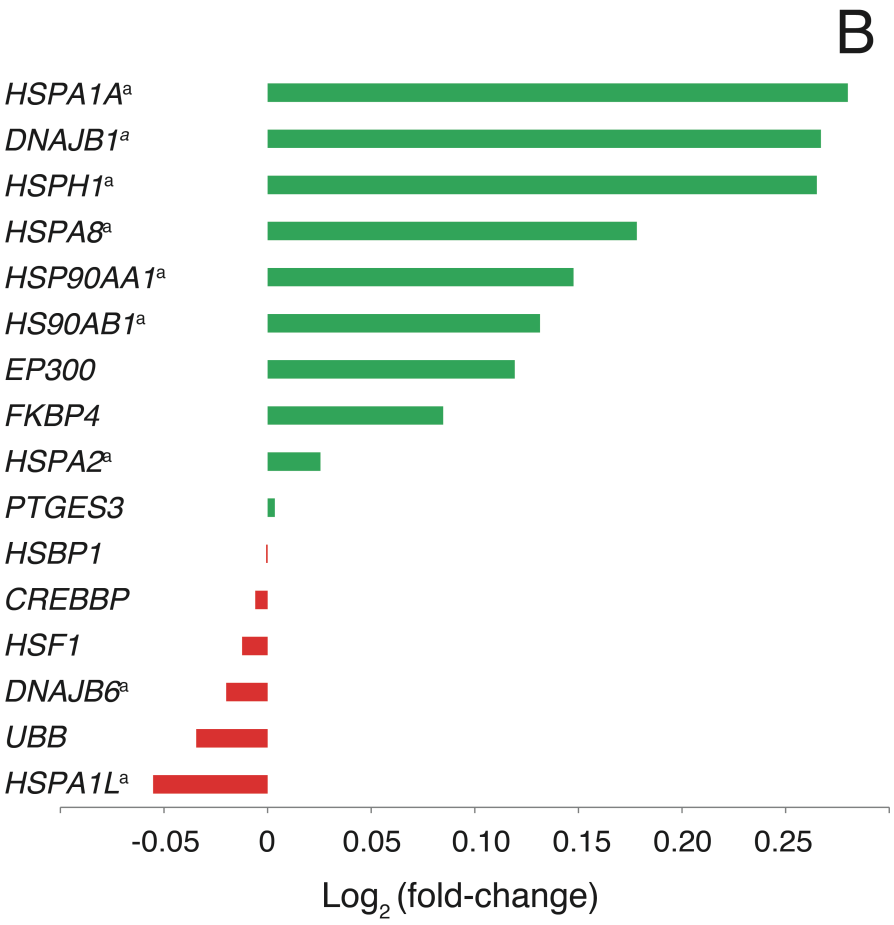
B
HSPA1A[a]
DNAJB1[a]
HSPH1[a]
HSPA8[a]
HSP90AA1[a]
HS90AB1[a]
EP300
FKBP4
HSPA2[a]
PTGES3
HSBP1
CREBBP
HSF1
DNAJB6[a]
UBB
HSPA1L[a]
-0.05
0
0.05
0.10
0.15
0.20
0.25
Log2 (fold-change)

Figure. 3. “Attenuation phase” is a representative pathway upregulated by molecular hydrogen, which are detected by GSEA (FCS) (↑$G1_c$ in Table 3 and Fig. 2) and PRS (PTA) (↑$P4_c$ in Table 6 and Fig. 2) with cross-platform analysis. “Attenuation phase” is a subset pathway of the heat shock response. **(A)** A diagram showing the interaction of genes in “attenuation phase”. Genes up- and down-regulated by molecular hydrogen are indicted by green and red symbols, respectively. **(B)** A bar graph showing difference in expression of genes in “attenuation phase” by molecular hydrogen. [a]Genes encoding heat shock proteins (HSPs).

Table 1. Numbers of statistically significant pathways

	Class	Analytical methods	Cross-platform analysis	Conventional meta-analysis
1	ORA	HGT	14 (up), 3 (down)	0
2	FCS	GSEA	9 (up), 9 (down)	1 (up), 8 (down)
3a	PTA	SPIA	1[a]	-[b]
3b	PTA	Clipper	6[a]	-[b]
3c	PTA	PRS	9 (up)	0
3d	PTA	DEGraph	0	-[b]
3e	PTA	TopologyGSA	0	-[b]
3f	PTA	TAPPA	0	-[b]
3g	PTA	PWEA	0	-[b]

The numbers and letters in the leftmost column represent labels used in the subtitles in Results. “Up” and “down” indicate the numbers of up- and down-regulated pathways, respectively. [a]SPIA and Clipper are designed to analyze up and down-regulated pathways simultaneously. [b]Conventional meta-analysis could not be applied to analytical methods in the class of PTA except for PRS (PTA) (see Materials and Methods for details).

Table 2. Top-ranked pathways comprised of up- and down-regulated genes detected with pathway analysis 1: HGT (cross-platform analysis)

Rank	Pathway	*p*-value	*q*-value
Upregulated pathways			
$\uparrow H1_c$	Collagen biosynthesis and modifying enzymes[a]	2.22E-05	0.002
$\uparrow H2_c$	Collagen formation[a]	2.48E-05	0.002
$\uparrow H3_c$	Vesicle-mediated transport	1.55E-04	0.007
$\uparrow H4_c$	Binding and uptake of ligands by scavenger receptors	7.27E-04	0.024
$\uparrow H5_c$	Extracellular matrix organization	8.80E-04	0.024
$\uparrow H6_c$	Assembly of collagen fibrils and other multimeric structures[a]	0.0016	0.036
$\uparrow H7_c$	Cellular response to heat stress[b]	0.0020	0.038
$\uparrow H8_c$	Clathrin derived vesicle budding	0.0029	0.044
$\uparrow H9_c$	trans-Golgi network vesicle budding	0.0029	0.044
$\uparrow H10_c$	Regulation of HSF1-mediated heat shock response[b]	0.0033	0.044
$\uparrow H11_c$	Cellular responses to stress	0.0048	0.059
$\uparrow H12_c$	HSF1-dependent transactivation[b]	0.0076	0.086
$\uparrow H13_c$	Glucose transport	0.0101	0.105
$\uparrow H14_c$	Membrane trafficking	0.0129	0.125
Downregulated pathways			
$\downarrow H1_c$	Cyclin D associated events in G1[c]	0.0030	0.078
$\downarrow H2_c$	G1 Phase[c]	0.0030	0.078
$\downarrow H3_c$	Mitotic G1-G1/S phases[c]	0.0060	0.102

Pathways are indicated in descending order of statistical significance. Pathway symbols used in Fig. 1 are indicated in the rank column. [a]Pathways in collagen biosynthesis; [b]Pathways in heat shock response; [c]Pathways in cell cycle.

Table 3. Top-ranked up- and down-regulated pathways detected with pathway analysis 2: GSEA (cross-platform analysis)

Rank	Pathway	*p*-value	*q*-value
Upregulated pathways			
↑$G1_c$	Attenuation phase[a]	< 0.0010	0.002
↑$G2_c$	HSF1-dependent transactivation[a]	< 0.0010	0.017
↑$G3_c$	Cellular response to heat stress[a]	< 0.0010	0.040
↑$G4_c$	Binding and uptake of ligands by scavenger receptors	< 0.0010	0.069
↑$G5_c$	Collagen biosynthesis and modifying enzymes[b]	< 0.0010	0.076
↑$G6_c$	Glucose transport	< 0.0010	0.101
↑$G7_c$	Regulation of gene expression in late stage (branching morphogenesis) pancreatic bud precursor cells	0.0039	0.102
↑$G8_c$	Regulation of HSF1-mediated heat shock response[a]	0.0018	0.103
↑$G9_c$	Collagen formation[b]	< 0.0010	0.116
Downregulated pathways			
↓$G1_c$	E2F mediated regulation of DNA replication[c]	< 0.0010	0.011
↓$G2_c$	Chromosome maintenance[c]	< 0.0010	0.046
↓$G3_c$	G1/S-specific transcription[c]	< 0.0010	0.065
↓$G4_c$	Telomere c-strand (lagging strand) synthesis[c]	< 0.0010	0.106
↓$G5_c$	Telomere c-strand synthesis initiation[c]	< 0.0010	0.110
↓$G6_c$	Nucleosome assembly[c]	< 0.0010	0.115
↓$G7_c$	BH3-only proteins associate with and inactivate anti-apoptotic bcl-2 members	0.0021	0.115
↓$G8_c$	TP53 regulates transcription of genes involved in G1 cell cycle arrest	< 0.0010	0.119
↓$G9_c$	CDC6 association with the ORC:origin complex[c]	0.0022	0.123

Pathways are indicated in descending order of statistical significance. Pathway symbols used in Fig. 1 are indicated in the rank column. [a]Pathways in heat shock response; [b]Pathways in collagen biosynthesis; [c]Pathways in cell cycle.

Table 4. Top-ranked up- and down-regulated pathways detected with pathway analysis 2: GSEA (conventional meta-analysis)

Rank	Pathway	*p*-value
Upregulated pathway		
$\uparrow G1_m$	Regulation of cholesterol biosynthesis by SREBP (SREBF)	5.09E-07
Downregulated pathways		
$\downarrow G1_m$	Cell cycle, mitotic	2.36E-07
$\downarrow G2_m$	Cell cycle checkpoints	3.41E-07
$\downarrow G3_m$	M phase	2.28E-06
$\downarrow G4_m$	G2/M checkpoints	6.20E-06
$\downarrow G5_m$	Mitotic G1-G1/S phases	8.50E-06
$\downarrow G6_m$	Cell cycle	1.48E-05
$\downarrow G7_m$	G1/S transition	2.33E-05
$\downarrow G8_m$	Mitotic prophase	5.33E-05

Pathways are indicated in descending order of statistical significance. Pathway symbols used in Fig. 1 are indicated in the rank column. *p*-value threshold < 5.43E-5 (= 0.05/920) after Bonferroni correction.

Table 5. Pathways detected with pathway analysis 3b: Clipper (cross-platform analysis)

Rank	Pathway	α_{mean}	α_{var}
$C1_c$	Glycosphingolipid metabolism	< 0.01	0.03
$C2_c$	The activation of arylsulfatases	0.01	0.02
$C3_c$	PTM: gamma carboxylation, hypusine formation and arylsulfatase activation	0.04	< 0.01
$C4_c$	Activation of genes by ATF4	0.04	0.01
$C5_c$	Synthesis, secretion, and inactivation of glucose-dependent insulinotropic polypeptide (GIP)	0.02	0.04
$C6_c$	Unfolded protein response	0.04	0.03

Pathways are indicated in descending order of statistical significance. Pathway symbols used in Fig. 1 are indicated in the rank column. α_{mean} is *p*-value for the mean which is calculated on the basis of graphical Gaussian model. α_{var} is *p*-value for the inverse covariance matrix which is calculated on the basis of graphical Gaussian model.

Table 6. Pathways detected with pathway analysis 3c: PRS (cross-platform analysis)

Rank	Pathway	nPRS	*p*-value	*q*-value
↑$P1_c$	Collagen biosynthesis and modifying enzymes[a]	20.9	< 0.0005	< 0.1
↑$P2_c$	Collagen formation[a]	18.6	< 0.0005	< 0.1
↑$P3_c$	HSF1-dependent transactivation[b]	14.8	< 0.0005	< 0.1
↑$P4_c$	Attenuation phase[b]	13.9	< 0.0005	< 0.1
↑$P5_c$	Scavenging by class F receptors	10.6	< 0.0005	< 0.1
↑$P6_c$	Regulation of gene expression in late stage (branching morphogenesis) pancreatic bud precursor cells	10.5	< 0.0005	< 0.1
↑$P7_c$	Cellular response to heat stress[b]	9.4	< 0.0005	< 0.1
↑$P8_c$	Regulation of HSF1-mediated heat shock response[b]	9.0	< 0.0005	< 0.1
↑$P9_c$	Assembly of collagen fibrils and other multimeric structures[a]	7.1	< 0.0005	< 0.1

Pathways are indicated in descending order of nPRS. Pathway symbols used in Fig. 1 are indicated in the rank column. nPRS represents how much the pathway is changed. [a]Pathways in collagen biosynthesis. [b]Pathways in heat shock response.

Supplementary Table 1. Microarray datasets

Dataset	Species	Tissue	Company	Platform
#1	mouse	liver	Affymetrix	GeneChip Mouse Gene 1.0 ST Array
#2	rat	liver	Affymetrix	HT RG-230 PM Array
#3	rat	liver	Affymetrix	Rat Expression 230A Array

Supplementary Table 2. Gene expression ratios for HSP47

Gene Symbol	$\log_2$ (fold-change)
SERPINH1	0.093

Supplementary Table 3. Gene expression ratios for collagen I-V

Gene Symbol	$\log_2$ (fold-change)
COL1A1	0.096
COL1A2	0.17
COL2A1	0.050
COL3A1	0.097
COL4A1	0.20
COL4A2	0.057
COL4A4	-0.023
COL1A5	0.15
COL4A6	0.043
COL5A1	0.097
COL5A2	0.11

Genes for collagen I-V were upregulated by hydrogen ($p = 0.0044$ by Wilcox rank sum test).

Supplementary Table 4. Gene expression ratios for HSP70 expressed in the liver

Gene Symbol	$\log_2$ (fold-change)
HSPA1A	0.28
HSPA1B	0.33
HSPA2	0.026
HSPA5	0.034
HSPA8	0.18
HSPA9	0.066

HSP70 family genes [1] were upregulated by hydrogen (p = 0.028 by Wilcox rank sum test).

Supplementary Table 5. Gene expression ratios for HSP90 expressed in the liver

Gene Symbol	$\log_2$ (fold-change)
HSP90AA1	0.15
HSP90AB1	0.13
HSP90B1	-0.040
TRAP1	-0.039

HSP90 family genes [2] were upregulated by hydrogen (p = 0.47 by Wilcox rank sum test).

References for Supplementary Tables

1. Daugaard M, Rohde M, Jaattela M. The heat shock protein 70 family: Highly homologous proteins with overlapping and distinct functions. FEBS Lett [Internet]. 2007;581:3702–10. Available from: http://www.ncbi.nlm.nih.gov/pubmed/17544402
2. Chen B, Piel WH, Gui L, Bruford E, Monteiro A. The HSP90 family of genes in the human genome: Insights into their divergence and evolution. Genomics. 2005;86:627–37.